Catalytic Alkyne and Diyne Metathesis with Mixed Fluoroalkoxy-Siloxy Molybdenum Alkylidyne Complexes

Manuel L. Zier, Sophie Colombel-Rouen, Henrike Ehrhorn, Dirk Bockfeld, Yann Trolez, Marc Mauduit, Matthias Tamm

Catalytic Alkyne and Diyne Metathesis with Mixed Fluoroalkoxy-Siloxy Molybdenum Alkylidyne Complexes

Manuel L. Zier,[a] Sophie Colombel-Rouen,[b] Henrike Ehrhorn,[a] Dirk Bockfeld,[a] Yann Trolez, [b] Marc Mauduit, [b] Matthias Tamm[a,*]

[a] Institut für Anorganische und Analytische Chemie, Technische Universität Braunschweig, Hagenring 30, 38106 Braunschweig

[b] Univ Rennes; Ecole Nationale Supérieure de Chimie de Rennes, CNRS, ISCR – UMR 6226, F-35000 Rennes, France

alkyne metathesis, alkynes, diynes, fluoroalkoxides, siloxides, molybdenum, metallacyclobutadienes

ABSTRACT: The reaction of the molybdenum alkylidyne complex [MesC≡Mo{OC(CF$_3$)$_3$}$_3$] (**MoF9**, Mes = 2,4,6-trimethylphenyl) with the potassium siloxides KOSi(O*t*Bu)$_3$ and KOSi(O*t*Bu)$_2$(OMes) furnished the mixed fluoroalkoxy-siloxy alkylidyne complexes [MesC≡Mo{OC(CF$_3$)$_3$}$_2${OSi(O*t*Bu)$_3$}] (**MoSiF9**) and [MesC≡Mo{OC(CF$_3$)$_3$}$_2${OSi(O*t*Bu)$_2$(OMes)}] (**MoSi*F9**). Treatment of **MoF9**, **MoSiF9** and **MoSi*F9** with an excess of 3-hexyne (EtC≡CEt) afforded labile metallacyclobutadiene (MCBD) complexes with a (C$_3$Et$_3$)Mo core, which are in equilibrium with the corresponding propylidyne (EtC≡Mo) complexes in solution. Thermodynamic parameters for these [2+2]-cycloaddition/cycloreversion reactions were determined by van 't Hoff plots, revealing that the nature of the ancillary siloxide ligand exerts a significant effect on the MCBD stability. X-ray diffraction analysis of **MoSi*F9-MCBD** provided the first accurate crystal structure of a molybdenacyclobutadiene (MoCBD). **MoF9**, **MoSiF9** and **MoSi*F9** proved active catalysts for the metathesis of internal alkynes and diynes, with **MoSi*F9** showing unprecendented selectivity in the conversion of sterically encumbered 1,3-pentadiynes into symmetrical 1,3,5-triynes and 2-butyne.

INTRODUCTION

Alkyne metathesis is an organic reaction that entails the redistribution of carbon-carbon triple bonds in the presence of transition metal alkylidyne complexes through the reversible formation of metallacyclobutadienes (MCBDs).[1] Shortly after its initial discovery in 1968, which involved the heterogeneously catalyzed "disproportionation" of 2-pentyne into 2-butyne and 3-hexyne,[2] the first homogeneous catalyst for the metathesis of alkynes was generated from a mixture of Mo(CO)$_6$ and the phenol reagent resorcinol.[3] With the discovery of the first SCHROCK-type tungsten and molybdenum alkylidyne complexes,[4] the suitability of molecular catalysts such as [*t*BuC≡W(O*t*Bu)$_3$][5,6] and [*t*BuC≡Mo(OC(CF$_3$)$_2$Me)$_3$][7] for alkyne metathesis was soon revealed. Ever since, fluoroalkoxide-supported alkylidyne complexes have played a prominent role,[8–10] and it was demonstrated that the degree of fluorination is crucial for optimum catalytic performance, with the less electrophilic molybdenum requiring a higher degree of fluorination.[11,12]

With the rise of alkyne metathesis in recent years,[13] alkylidyne complexes bearing fluoroalkoxide ligands have again played an important role in the development of this area.[14,15] In accordance with the above findings, the catalytic activity of the molybdenum 2,4,6-trimethylbenzylidyne complexes [MesC≡Mo{OC(CF$_3$)$_n$Me$_{3-n}$}$_3$] (**MoF0**, *n* = 0; **MoF3**, *n* = 1; **MoF6**, *n* = 2; **MoF9**, *n* = 3) can be tuned by varying the degree of fluorination,[16] whereby **MoF6** has the highest catalytic activity and can even be used for the metathesis of terminal alkynes (Figure 1).[17,18]

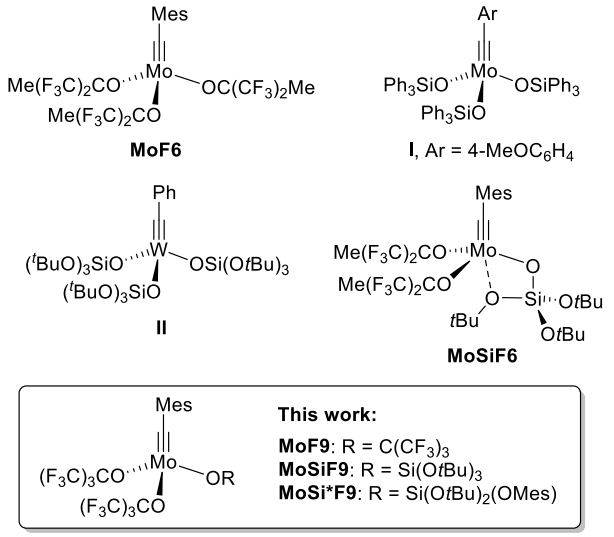

Figure 1. Selected fluoroalkoxide- and siloxide-supported alkyne metathesis catalysts; Mes = 2,4,6-trimethylphenyl.

In case of tungsten, a lower degree of fluorination is sufficient, and [MesC≡W{OC(CF$_3$)Me$_2$}$_3$] (**WF3**) is arguably the most active tungsten-based alkyne metathesis catalyst reported to date.[16,19] Convenient access to these complexes was provided by the development of reliable protocols for their preparation from Mo(CO)$_6$ or W(CO)$_6$, respectively,[20,21] which also furnished **MoF6**-type initiators for ring-opening alkyne metathesis polymerization

(ROAMP)[22–24] as well as N-heterocyclic carbene (NHC) adducts of related molybdenum and tungsten benzylidyne complexes.[25–28] Recently, related molybdenum benzylidyne complexes were even used for olefin metathesis reactions.[29]

Siloxide-supported alkylidyne complexes are another important class of alkyne metathesis catalysts,[30] and the triphenylsiloxy molybdenum complex **I** is probably the most frequently used species,[31,32] in particular for natural product synthesis through ring-closing alkyne metathesis (RCAM).[33–43] Recently, molybdenum alkylidyne complexes with arene-bridged tripodal siloxide ligands were introduced and employed as alkyne metathesis catalysts with improved functional group tolerance.[44–47] This design strategy is somewhat reminiscent of molybdenum alkylidyne complexes with tripodal tris(aryloxide) ligands,[48] which were used extensively in polymer and supramolecular chemistry,[49–53] and more recently, for alkyne metathesis operating under open air conditions.[54]

Another important ancillary ligand is tri(*tert*-butoxy)siloxide, $(t\text{BuO})_3\text{SiO}$, which was used for the preparation of the tungsten benzylidyne complex **II** (Figure 1).[55,56] This complex proved active not only in alkyne metathesis, but was also employed for the homo- and cross-metathesis of 1,3-diynes (Scheme 1).[57–59] The high selectivity towards diyne formation can be rationalized by the so-called α,α-mechanism that involves alkynylalkylidyne complexes (M≡CC≡CR) as catalytically active species and α,α-dialkynyl-metallcyclobutadiene (MCBD) intermediates. The disproportionation into monoynes and triynes, which was observed as a very slow side reaction, can then be explained by deviation from this mechanism through formation of α,β-dialkynyl-MCBDs, with α and β referring to the 1,3- and 2-positions, respectively, of the carbon atoms in a four-membered metallacycle. These mechanistic considerations could be substantiated experimentally and theoretically,[57,59] and a fluoroalkoxide-supported α,α-diethynyl-tungstenacyclobutadiene complex was recently isolated and structurally characterized by single-crystal X-ray diffraction.[60] While diyne cross-metathesis (DYCM) can certainly be regarded as a convenient new method for the preparation of unsymmetrical diynes, the selective disproportion of diynes into monoynes and triynes represents a highly interesting reaction in its own right, since it would provide a straightforward way to synthesize compounds with the highly desirable 1,3,5-hexatriyne core (Scheme 1). In fact, an expedient synthesis of conjugated triynes from sterically hindered 1,3-pentadiynes, e.g. with R = $i\text{Pr}_3\text{Si}$ and R' = Me, in the presence of catalyst **I** was recently reported. Nevertheless, less sterically demanding groups, e.g. R = Mes, furnished a considerable drop of selectivity with lower triyne/diyne ratios, leaving the quest for more efficient catalysts with higher selectivity and productivity.[61]

The tri(*tert*-butoxy)siloxide ligand was also employed for the preparation of the mixed fluoroalkoxy-siloxy complex **MoSiF6** (Figure 1), which served as a model complex for the silica-supported catalyst **MoF6@SiO$_2$**. The homogeneous catalyst **MoF6** and its immobilized form **MoF6@SiO$_2$** showed unprecedented catalytic activity at parts-per-million loadings; however, lower activity was observed for the heterogeneous system, presumably owing to the rigidity of the surface species.[62] Noteworthy, the molecular catalysts **MoF6** and **MoSiF6** showed comparable activity in the self-metathesis of 1-phenyl-1-propyne, revealing that the replacement of one fluroalkoxide by the $(t\text{BuO})_3\text{SiO}$ group does not lead to a deterioration in the catalytic activity.[63] The X-ray crystal structure of **MoSiF6** showed that the siloxide is bound in a chelating κ^2*O,O'* fashion in the solid state. This interaction might be favorable to stabilize the catalyst and also relevant stationary structures during alkyne metathesis, since similar interactions were found computationally for the diyne metathesis reaction in the presence of **II**.[59]

Scheme 1. Metathesis Reactions with Alkynes and 1,3-Diynes

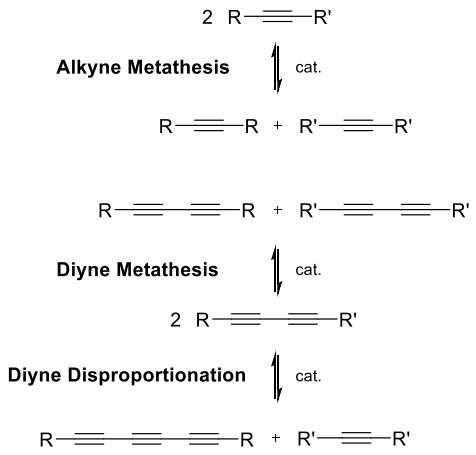

We envisaged that introduction of the $(t\text{BuO})_3\text{SiO}$ group could be generally used to fine-tune the electronic and catalytic properties of fluoroalkoxide-supported catalyst systems and that further variation of the siloxide ligand, as for instance in unsymmetrical $(\text{MesO})(t\text{BuO})_2\text{SiO}$, might allow further adjustment of the substrate-specific selectivity.[64] This concept was first applied to **MoF9**, which had proven to be a valuable catalyst for the metathesis of internal alkynes.[16] In preliminary studies, it also demonstrated reactivity towards symmetrical diynes, however, with a stronger tendency to form a mixture of diynes, triynes and even tetraynes.[65] Therefore, we present herein the preparation and characterization of the siloxy derivatives **MoSiF9** and **MoSi*F9** and their application, together with **MoF9**, in the metathesis of alkynes and diynes (Scheme 1). To rationalize their performance in alkyne metathesis, we also aimed at the isolation of molybdenacyclobutadiene (MoCBD) complexes and have assessed their stability by variable-temperature NMR and computational studies.

RESULTS AND DISCUSSION

Preparation and Characterization of Mixed Fluoroalkoxy-Siloxy Molybdenum Alkylidyne Complexes. The mixed fluoroalkoxy-siloxy complex **MoSiF6** had been prepared by a one-pot synthesis from $[\text{MesC}{\equiv}\text{MoBr}_3(\text{dme})]$ by reaction with two equivalents of $\text{KOC}(\text{CF}_3)_2\text{Me}$ and one equivalent of $\text{KOSi}(\text{O}t\text{Bu})_3$.[63] This route proved unfavorable

in the case of **MoSiF9**, affording a mixture of mono- and disiloxy complexes; see Figure S40 in the Supporting Information for the X-ray crystal structure of [MesC≡Mo{OC(CF$_3$)$_3$}{OSi(O*t*Bu)$_3$}$_2$]. Alternatively, **MoSiF9** was prepared following the route established for imidazolin-2-iminato complexes.[20,66–68] Thus, it was isolated in significantly higher yield (93%) by treatment of **MoF9** with one equivalent of KOSi(O*t*Bu)$_3$ and substitution of one OC(CF$_3$)$_3$ moiety (Scheme 2). Unfortunately, both routes failed to give pure **MoSiF0** and **MoSiF3**, which were only characterized by X-ray diffraction analysis (Figures S37 and S38). Since these complexes are unlikely to act as suitable catalysts,[16,63] we decided not to optimize their synthesis. For the preparation of **MoSi*F9**, the unsymmetrical silanol (MesO)(*t*BuO)$_2$SiOH was obtained in four steps from SiCl$_4$ according to the literature.[64] Reaction with KH gave the potassium salt KOSi(O*t*Bu)$_2$(OMes), which was treated with **MoF9** to furnish **MoSi*F9** in moderate yield (56%) after recrystallization (Scheme 2).

Scheme 2. Synthesis of Mixed Fluoroalkoy-Siloxy Molybdenum Benzylidyne Complexes

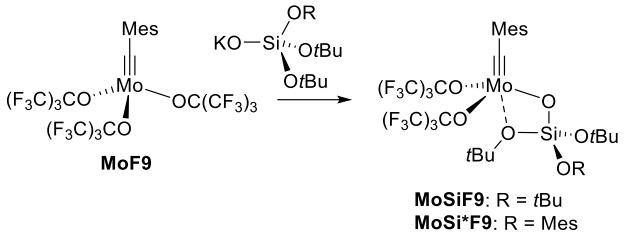

The NMR spectra of **MoSiF9** and **MoSi*F9** were recorded in C$_6$D$_6$. The ^{1}H NMR spectrum of **MoSiF9** exhibits one singlet for the *t*Bu hydrogen atoms together with three signals for the hydrogen atoms of the Mes substituent, while the spectrum of **MoSi*F9** shows three additional signals for the mesityloxy (MesO) group, revealing C_s symmetry in solution at room temperature on the NMR time-scale. Accordingly, one singlet is found in each ^{19}F NMR spectrum at –72.9 ppm (**MoSiF9**) and –73.1 ppm (**MoSi*F9**), respectively, which falls in the same range as for **MoF9** (73.7 ppm). In the ^{13}C NMR spectra, the carbyne carbon atoms give rise to characteristic lowfield signals at 320.9 ppm (**MoSiF9**) and 323.5 ppm (**MoSi*F9**), which is at higher field compared to 332.7 ppm in **MoF9**. Likewise, a highfield shift had been observed from 317.6 ppm in **MoF6** to 306.6 ppm in **MoSiF6** upon introduction of the less electron-withdrawing siloxide ligands.[63]

The molecular structures of **MoSiF9** and **MoSi*F9** could be established by X-ray diffraction analysis; an ORTEP diagram of the latter is shown in Figure 2. The molecular structures of **MoSiF*n*** (*n* = 0, 3, 9) are presented in Figures S37, S38 and S39, and pertinent structural data of all complexes **MoSiF*n*** (*n* = 0, 3, 6, 9) and **MoSi*F9** are assembled in Table 1. All complexes show strongly distorted tetrahedral geometries around the metal atoms with short Mo–C1 bond length of ca. 1.75 Å and large Mo–C1–C2 angles (≥172°) in a similar range as reported for MoFn (n = 0, 3, 6, 9).[16] In all complexes, the siloxide ligand binds in a chelating κ^2*O*,*O'* fashion and, in addition to a short Mo–O1 bond of ca. 1.92 Å, provides a significantly longer Mo–O2 distance, which decreases from 2.742(1) Å in **MoSiF0** to 2.506(3) Å in **MoSiF9** with the increasing number of fluorine atoms. This coordination mode is often found in rare earth metal siloxides,[69] and only recently, it has been established for several complexes derived from the homoleptic Mo(III) complex [Mo{OSi(O*t*Bu)$_3$}$_3$].[70] Since the additional coordination through one of the O*t*Bu groups renders **MoSi*F9** C_1-symmetric, a variable-temperature NMR Study was performed. Below a coalescence temperature of ca. –90 °C, two singlets start to get resolved for the *t*Bu groups by ^{1}H NMR spectroscopy, suggesting overall fast dynamics and a weak secondary molydenum-oxygen interaction (Figures S15).

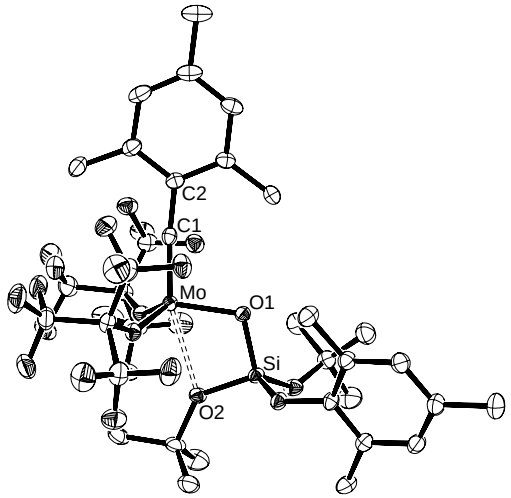

Figure 2. ORTEP diagram of **MoSi*F9** with thermal displacement parameters drawn at 30% probability; hydrogen atoms are omitted for clarity.

Table 1. Selected Bond Lengths [Å] and Angles [°] of Complexes MoSiF*n* (*n* = 0, 3, 6, 9)

	M–C1	Mo–O2	M–C1–C2
MoSiF0	1.7523(14)	2.7420(10)	173.03(12)
MoSiF3	1.7571(18)	-[a]	172.00(15)
MoSiF6[b]	1.755(3)	2.5734(16)	173.5(2)
MoSiF9	1.748(5)	2.506(3)	172.3(4)
MoSi*F9	1.754(3)	2.5376(17)	173.6(2)

[a] Disordered O*t*Bu group. [b] From ref. [63].

Preparation and Characterization of Molybdenacyclobutadiene Complexes. Despite the importance of molybdenum alkylidyne complexes in alkyne metathesis, examples of structurally characterized molybdenacyclobutadienes (MoCBD) are still rare,[71] and early examples were only characterized in solution by NMR spectroscopy.[7,12,72] A few 1,3-diamino-substituted MoCBDs were recently obtained, which have diamagnetic or paramagnetic ground states depending on the amino substituents.[24,73] Related to this study, we reported the MoCBDs derived from the reactions of **MoF6** and **MoF9** with an excess of 3-hexyne. Unfortunately, the crystallographic characterization of the resulting complexes [(C$_3$Et$_3$)Mo{OC(CF$_3$)$_2$Me}$_3$] (**MoF6-MCBD**)

and [(C_3Et_3)Mo{$OC(CF_3)_3$}$_3$] (**MoF9-MCBD**) suffered from disorder, precluding an accurate discussion of the structural parameters.[16,60] Gratifyingly, this has recently been possible for [(C_3Et_3)Mo($OSiPh_3$)$_3$], which provided pertinent information about the structure of an MoCBD in the solid state.[74] Since the presence of the siloxide ligands in **MoSiF9** and **MoSi*F9** might be favorable to reduce crystallographic disorder associated with fluoroalkoxide ligands, we aimed at isolating similar MoCBD complexes from their reaction with an excess of 3-hexyne (Scheme 3).

Scheme 3. Preparation of Molybdenaclobutadienes

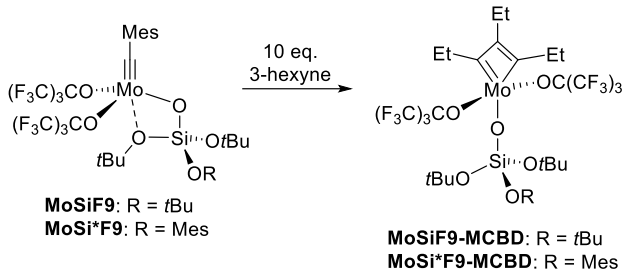

In case of **MoSiF9**, addition of 10 equivalents of 3-hexyne to a saturated *n*-pentane solution at –38 °C produced an immediate characteristic color change from yellow to purple, and **MoSiF9-MCBD** could be isolated as purple crystals by storing this solution in the refrigerator at –38 °C for a couple of days. X-ray diffraction analysis confirmed the formation of the expected metallacycle and provided a second examples of a high-quality MoCBD crystal structure (Figure 3). The environment around the Mo atom is best described as distorted square-pyramidal (SP) with C1 at the apex in agreement with a τ_5 value of 0.30 based on the two largest angles, *viz.* O5–Mo–O6 = 162.56(14)° and O1–Mo–C3 = 144.8(2)°.[75] The alternative description as trigonal-bipyramidal (TBP) is clearly less appropriate, as the angles O1–Mo–C1 and O1–Mo–C3 of 131.9(2)° and 144.8(2)° differ quite significantly. In agreement with the SP assignment, the Mo–C bond lengths of 1.877(5) Å (Mo–C1) and 1.924(6) Å (Mo–C3) are markedly different, and together with the C1–C2 and C2–C3 bond lengths of 1.480(8) Å and 1.424(8) Å, respectively, a short-long-short-long alternation of bond lengths within the MoC_3 ring is observed. In principle, these structural parameters are similar to those recently determined for [(C_3Et_3)Mo($OSiPh_3$)$_3$], however, with a τ_5 value of 0.37 and a slighly less pronounced bond alternation, this complex is even more distorted towards TBP.[74] This structure is usually associated with the transition state for MCBD interconversion, which involves inverting the SP structure and swapping the apical positions. It is also noteworthy that the siloxide ligand is no longer bound in a κ^2-fashion as found in the precursor **MoSiF9**, but features a short Mo–O1 bond lengths of 1.869(4) Å with an almost linear Mo–O1–Si arrangement of 173.3(2)°, revealing a significant degree of π-donation towards the Mo atom.

Purple crystals of **MoSi*F9-MCBD** were isolated as described above by storing a solution of **MoSi*F9** with 10 equivalents of 3-hexyne in *n*-pentane at –38 °C (Scheme 3). X-ray diffraction analysis provided another MoCBD structure, however, a modulation is observed that affords four independent molecules in the asymmetric unit. In addition, disorder could only be fully resolved in one of the four molecules, and the structural parameters should therefore be treated with caution. Crystallographic details and ORTEP presentations together with tentative bond lengths and angles can be found in the Supporting Information (Figure S41).

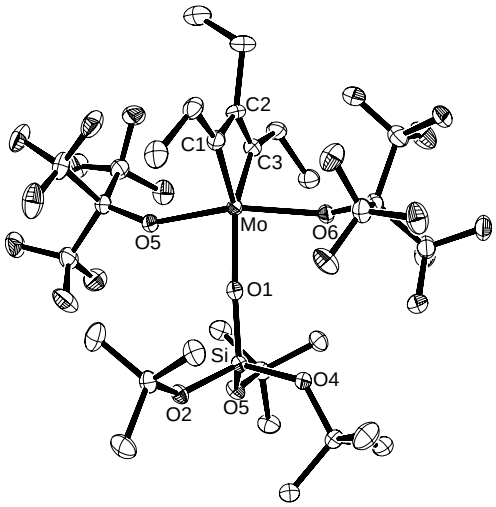

Figure 3. ORTEP diagram of **MoSiF9-MCBD** with thermal displacement parameters drawn at 30% probability; hydrogen atoms are omitted for clarity. Selected bond lengths [Å] and angles [°]: Mo–C1 1.877(5), Mo–C3 1.924(6), Mo–O1 1.869(4), Mo–O5 2.058(3), Mo–O6 2.053(3), C1–C2 1.480(8), C2–C3 1.424(8), Mo–O1–Si 173.3(2), O1–Mo–C1 131.9(2), O1–Mo–C3 144.8(2), O5–Mo–O6 162.56(14).

NMR spectroscopic characterization of both MCBD complexes revealed different stabilities in solution. Dissolving crystalline **MoSiF9-MCBD** in CD_2Cl_2 or toluene-d_8 leads to a fast decolorization; the characteristic pink color can be restored by cooling, which suggests the existence of an equilibrium with the alkylidyne complex **MoSiF9^{Et}** and 3-hexyne. Accordingly, the ^{1}H NMR spectra show almost exclusively the signals for the alkylidyne complex and 3-hexyne and one signal in the ^{19}F NMR spectra at room temperature. At lower temperatures, two ^{19}F NMR signals are observed, e.g., at –72.9 ppm and –72.0 ppm in toluene-d_8 at –40.7 °C, which can be assigned to the alkylidyne and MCBD species, respectively. In contrast, solutions of **MoSi*F9-MCBD** retain their characteristic pink color at room temperature, and the ^{19}F NMR spectrum in toluene-d_8 shows a major signal at –72.6 ppm for the MCBD complex together with a minor signal at –73.1 ppm for the alkylidyne complex in approx. 94:6 ratio, indicating a significantly higher stability of **MoSi*F9-MCBD** compared to **MoSiF9-MCBD**. MCBD formation could be confirmed in both cases by observation of characteristic lowfield ^{13}C NMR signals at 265.5 and 152.3 ppm (in CD_2Cl_2 at –39.6 °C for **MoSiF9-MCBD**) and at 265.1 and 151.1 ppm (in toluene-d_8 at room temperature for **MoSi*F9-MCBD**). These chemical shifts can be assigned to the α- and β-carbon atoms of the MoC_3 fragment and are in good agreement with the NMR data reported for other MoCBD complexes,[7,12,60,63,72] e.g., 269.9 and 156.0 ppm for **MoF9-MCBD**.[16]

The latter complex, **MoF9-MCBD**, could also be observed in solution at room temperature,[16] indicating a significant higher stability compared to **MoSiF9-MCBD** and a similar stability compared to **MoSi*F9-MCBD**. To analyze this surprisingly different behavior, variable-temperature NMR studies were performed. For this purpose, the crystalline MCBD complexes were dissolved in toluene-d_8, and their reversible [2+2]-cycloreversion/-cycloaddition reactions involving equimolar amounts of 3-hexyne and the respective propylidyne complex were monitored by ^{19}F NMR spectroscopy. The corresponding equilibrium constants K = [MCBD]/[alkylidyne]^2 were determined in a broad temperature range (> 50 K), and van 't Hoff analysis provided the thermodynamic data shown in Table 2 (see also the Supporting Information for details). For the pair **MoF9^{Et}/MoF9-MCBD**, the parameters of $\Delta H°$ = −21.4(2) kcal mol^{-1}, $\Delta S°$ = −80(1) cal mol^{-1} K^{-1} were obtained, which indicate a fairly exothermic reaction in agreement with MCBD stabilization in the presence of three electron-withdrawing OC(CF$_3$)$_3$ ligands. However, reversibility of MCBD formation is ensured by the significant decrease in entropy, affording an only slightly exergonic reaction with $\Delta G°$ = −2.4(1) kcal mol^{-1} in agreement with the observation of **MoF9-MCBD** at room temperature.

In contrast, the **MoSiF9^{Et}/MoSiF9-MCBD** system generates the parameters of $\Delta H°$= −18.7(7) kcal mol^{-1} and $\Delta S°$ = −87(3) cal mol^{-1} K^{-1} for an appreciably endergonic reaction with $\Delta G°$ = +7.4(1) kcal mol^{-1}, revealing a significant destabilization of **MoSiF9-MCBD** by introduction of the OSi(O*t*Bu)$_3$ ligand, both by enthalpic and entropic contributions. These differences could be ascribed to a weaker electron-withdrawing nature of the siloxide in comparison with the fluoroalkoxide ligand and to a more ordered MCBD complex, in which the siloxide ligand is aligned with the four-membered metallacycle. The presence of the more asymmetric siloxide ligand OSi(O*t*Bu)$_2$(OMes) in the **MoSi*F9^{Et}/MoSi*F9-MCBD** system renders MCBD formation favorable again, with the parameters of $\Delta H°$ = −20.8(3) kcal mol^{-1} and $\Delta S°$ = −77(1) cal mol^{-1} K^{-1} affording an overall exergonic reaction with $\Delta G°$= −2.3(1) kcal mol^{-1}. These findings indicate that subtle differences in the ligand design exert a significant impact on the thermodynamics of MCBD formation, which enables fine-tuning of the catalytic activity by avoiding unfavorably strong stabilization or destabilization of the MCBD intermediate. Furthermore, variation of the ancillary ligands may affect the selectivity of the alkylidyne complexes in catalytic alkyne and diyne metathesis, and these studies are presented in the following.

Table 2. Experimental Thermodynamic Parameters for the Formation of Metallacyclobutadiene Complexes

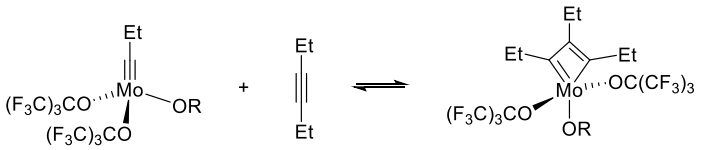

alkylidyne	MCBD	OR	$\Delta H°$ [kcal/mol][a]	$\Delta S°$ [cal/mol K][a]	$\Delta G°$ [kcal/mol][a]
MoF9^{Et}	**MoF9-MCBD**	OC(CF$_3$)$_3$	−21.4(2)	−80(1)	−2.4(1)
MoSiF9^{Et}	**MoSiF9-MCBD**	OSi(O*t*Bu)$_3$	−18.7(7)	−87(3)	+7.4(1)
MoSi*F9^{Et}	**MoSi*F9-MCBD**	OSi(O*t*Bu)$_2$(OMes)	−20.8(3)	−77(1)	−2.3(1)

[a] Enthalpies ($\Delta H°$), entropies ($\Delta S°$) and Gibbs free energies at 298.15 K ($\Delta G°$).

Catalytic Alkyne and Diyne Metathesis. The catalytic performance of **MoSiF9** and **MoSi*F9** in alkyne metathesis was investigated for a couple of standard test substrates (Scheme 4), which had also been previously employed with the catalysts **MoF*n*** (n = 0, 3, 6, 9). The results are summarized in Table 3, including also those previously obtained with **MoF9**.[16] It should be noted that **MoSiF9** and **MoSi*F9** proved inactive in terminal alkyne metathesis and produced polymeric material as also observed for **MoF9**. In contrast excellent catalytic performance was observed for internal alkynes. Thus, homometathesis of the ether **1** and the ester **3** proceeded in toluene with catalyst loadings of 1 mol% and in the presence of molecular sieves (MS 5 Å) as a 2-butyne scavenger, affording the corresponding products **2** and **4** in almost quantitative yields within two hours at room temperature. Similarly, RCAM of diester **5** gave the cyclic alkyne **6** in about 95% isolated yield, which exceeds the results previously reported with **MoF9** (76%).[16] 1-Phenylpropyne (**7**) was also almost completely converted to tolane (**8**). For all substrates, the conversion was also followed by gas chromatography, and the resulting conversion versus time diagrams indicate a higher activity of **MoSiF9** in comparison with the sterically more encumbered **MoSi*F9** (see Figures S43 and S44).

It could be suspected, however, that steric demand might affect the metathesis of diynes, which was reported recently to proceed with formation of triynes if sterically hindered 1,3-pentadiynes such as **9a** (R = Si*i*Pr$_3$ = TIPS) and **9b** (R = Mes) are employed. In the presence of **I** (3 mol%, 40 °C, 3 h), 1,6-bis(triisopropylsilyl)-1,3,5-hexatriyne (**10a**) formed with high selectivity over the corresponding symmetrical 1,3-butadiyne and could be isolated in 63% yield after silica gel chromatography. Significantly lower selectivity towards triyne formation was observed for other substrates such as **9b**, which afforded **10b** as a complex mixture with the corresponding diyne, tetrayne and possibly higher polyynes.[61] Hence, diyne disproportionation of **9a** and **9b** was investigated under similar conditions in the presence of **MoF9**, **MoSiF9** and **MoSi*F9** (Scheme 4). The reactions were performed at room temperature in toluene solution with

catalyst loadings of 1 mol%, and the addition of 5 Å as well as 4 Å molecular sieves (MS) was found to be favorable in line with the previous report. In case of **9a**, triyne **10a** formed with high selectivity for all three catalysts, with the GC traces showing the complete absence of the diyne *i*Pr$_3$SiC≡CC≡CSi*i*Pr$_3$. **MoSi*F9** showed the best performance, and **10a** could be isolated in 88% yield after a reaction time of 4 h at room temperature. In case of **9b**, the selectivity towards the formation triyne **10b** was also significantly higher than previously reported for catalyst **I**, which allowed its isolation in 71% by application of **MoSi*F9**. These results clearly prove the superiority of the catalyst **MoSi*F9** and allows to envisage the use of less hindered precursors than described previously, including highly-functionalized diynes.

Scheme 4. Alkyne and Diyne Metathesis Reactions

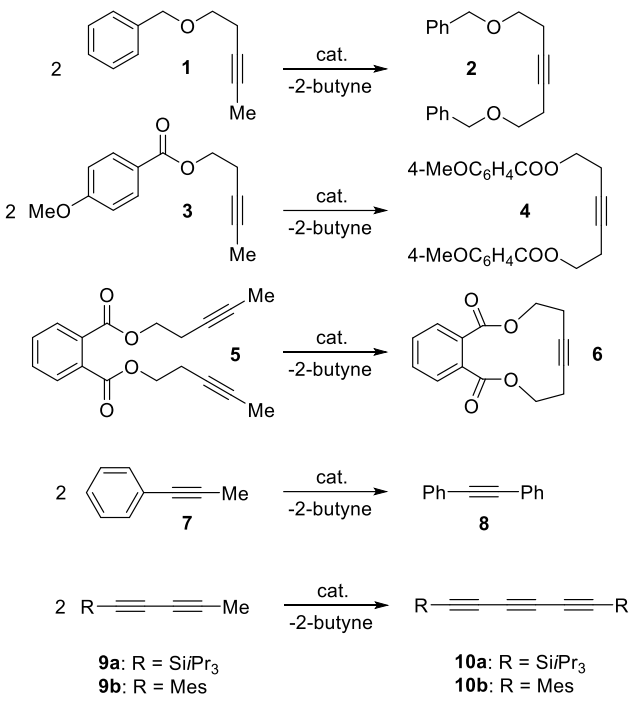

Table 3. Yields [%] of Alkyne and Diyne Metathesis Reactions[a]

Substrate/Product	**MoF9**	**MoSiF9**	**MoSi*F9**
1/**2**[a]	89	92	97
3/**4**[a]	92	99	99
5/**6**[b]	76	94	95
7/**8**[a]	78	96	88
9a/**10a**[c]	82	79	88
9b/**10b**[c]	50	17	71

[a] Homometathesis: Substrate 0.5 mmol, MS 5 Å 500 mg, catalyst 1 mol%, toluene (2.5 mL), 2 h, rt. [b] RCAM: Substrate 0.25 mmol, MS 5 Å 250 mg, catalyst 2 mol%, toluene (12 mL), 2 h, rt. [c] Diyne metathesis: Substrate 0.5 mmol, MS 4 Å 400 mg, MS 5 Å 400 mg, catalyst 1 mol%, toluene (2.5 mL), 4 h (**9a**), 1 h (**9b**), rt.

CONCLUSION

The preparation of mixed fluoroalkoy-siloxy molybdenum alkylidyne complexes provides an opportunity to fine-tune their activity and selectivity in catalytic alkyne and diyne metathesis reactions by variation of the ancillary siloxide ligand, which has a significant influence on the stability of the intermediate metallacyclobutadiene (MCBD) species. While the introduction of the symmetrical siloxide OSi(O*t*Bu)$_3$ turns **MoF9** into the superior alkyne metathesis catalyst **MoSiF9**, the introduction of the unsymmetrical siloxide OSi(O*t*Bu)$_2$(OMes) afforded **MoSi*F9**, which proved to be an excellent catalyst for the selective conversion of sterically encumbered 1,3-pentadiynes (RC≡CC≡CMe) into symmetrical 1,3,5-triynes (RC≡CC≡CC≡CR) and 2-butyne (MeC≡CMe). This reactivity will be further exploited with the goal to identify structure-activity and structure-selectivity relationships for a substrate-specific adjustment of the ancillary siloxide ligand, with the variation of the fluoroalkoxide ligands offering additional tuning options.

ASSOCIATED CONTENT

Supporting Information

This material is available free of charge via the Internet at http://pubs.acs.org

Full experimental details, NMR spectra and studies, crystallographic data and catalytic protocols.

Accession Codes

CCDC 2074892–2074898 contain the supplementary crystallographic data for this paper. These data can be obtained free of charge via www.ccdc.cam.ac.uk/data_request/cif, or by emailing data_request@ccdc.cam.ac.uk, or by contacting The Cambridge Crystallographic Data Centre, 12 Union Road, Cambridge CB2 1EZ, UK; fax: +44 1223 336033.

AUTHOR INFORMATION

Corresponding Author

*E-mail: m.tamm@tu-bs.de

ORCID

Matthias Tamm: 0000-0002-5364-0357

Dirk Bockfeld: 0000-0003-1084-8577

Yann Trolez: 0000-0002-5421-955

Marc Mauduit: 0000-0002-7080-9708

Sophie Colombel-Rouen: 0000-0003-2603-2783

Notes

The authors declare no competing financial interest.

ACKNOWLEDGMENT

YT and MM are grateful to the CNRS and the Ecole Nationale supérieure de chimie de Rennes for supporting this work. MT acknowledges support by the Deutsche Forschungsgemeinschaft through grant TA 189/12-2.

References

(1) Katz, T. J.; McGinnis, J. Mechanism of the olefin metathesis reaction. *J. Am. Chem. Soc.* **1975**, *97*, 1592–1594.

(2) Pennella, F.; Banks, R. L.; Bailey, G. C. Disproportionation of alkynes. *Chem. Commun.* **1968**, 1548.

(3) Mortreux, A.; Blanchard, M. Metathesis of alkynes by a molybdenum hexacarbonyl–resorcinol catalyst. *J. Chem. Soc., Chem. Commun.* **1974**, 786–787.

(4) Clark, D. N.; Schrock, R. R. Multiple metal-carbon bonds. 12. Tungsten and molybdenum neopentylidyne and some tungsten neopentylidene complexes. *J. Am. Chem. Soc.* **1978**, *100*, 6774–6776.

(5) Wengrovius, J. H.; Sancho, J.; Schrock, R. R. Metathesis of acetylenes by tungsten(VI)-alkylidyne complexes. *J. Am. Chem. Soc.* **1981**, *103*, 3932–3934.

(6) Sancho, J.; Schrock, R. R. Acetylene metathesis by tungsten(VI) alkylidyne complexes. *J. Mol. Catal.* **1982**, *15*, 75–79.

(7) McCullough, L. G.; Schrock, R. R. Multiple metal-carbon bonds. 34. Metathesis of acetylenes by molybdenum(VI) alkylidyne complexes. *J. Am. Chem. Soc.* **1984**, *106*, 4067–4068.

(8) Schrock, R. R. High-oxidation-state molybdenum and tungsten alkylidyne complexes. *Acc. Chem. Res.* **1986**, *19*, 342–348.

(9) Schrock, R. R. High oxidation state multiple metal-carbon bonds. *Chem. Rev.* **2002**, *102*, 145–179.

(10) Schrock, R. R. Alkyne metathesis by molybdenum and tungsten alkylidyne complexes. *Chem. Commun.* **2013**, *49*, 5529–5531.

(11) Freudenberger, J. H.; Schrock, R. R.; Churchill, M. R.; Rheingold, A. L.; Ziller, J. W. Metathesis of acetylenes by (fluoroalkoxy)tungstenacyclobutadiene complexes and the crystal structure of W(C3Et3)[OCH(CF3)2]3. A higher order mechanism for acetylene metathesis. *Organometallics* **1984**, *3*, 1563–1573.

(12) McCullough, L. G.; Schrock, R. R.; Dewan, J. C.; Murdzek, J. C. Multiple metal-carbon bonds. 38. Preparation of trialkoxymolybdenum(VI) alkylidyne complexes, their reactions with acetylenes, and the x-ray structure of Mo[C3(CMe3)2][OCH(CF3)2](C5H5N)2. *J. Am. Chem. Soc.* **1985**, *107*, 5987–5998.

(13) Fürstner, A. Alkyne metathesis on the rise. *Angew. Chem. Int. Ed.* **2013**, *52*, 2794–2819.

(14) Wu, X.; Tamm, M. Recent advances in the development of alkyne metathesis catalysts. *Beilstein J. Org. Chem.* **2011**, *7*, 82–93.

(15) Ehrhorn, H.; Tamm, M. Well-Defined Alkyne Metathesis Catalysts: Developments and Recent Applications. *Chem. Eur. J.* **2019**, *25*, 3190–3208.

(16) Bittner, C.; Ehrhorn, H.; Bockfeld, D.; Brandhorst, K.; Tamm, M. Tuning the Catalytic Alkyne Metathesis Activity of Molybdenum and Tungsten 2,4,6-Trimethylbenzylidyne Complexes with Fluoroalkoxide Ligands OC(CF 3) n Me 3–n (n = 0–3). *Organometallics* **2017**, *36*, 3398–3406.

(17) Haberlag, B.; Freytag, M.; Daniliuc, C. G.; Jones, P. G.; Tamm, M. Efficient metathesis of terminal alkynes. *Angew. Chem. Int. Ed.* **2012**, *51*, 13019–13022.

(18) Hötling, S.; Bittner, C.; Tamm, M.; Dähn, S.; Collatz, J.; Steidle, J. L. M.; Schulz, S. Identification of a Grain Beetle Macrolide Pheromone and Its Synthesis by Ring-Closing Metathesis Using a Terminal Alkyne. *Org. Lett.* **2015**, *17*, 5004–5007.

(19) Ehrhorn, H.; Schlösser, J.; Bockfeld, D.; Tamm, M. Efficient catalytic alkyne metathesis with a fluoroalkoxy-supported ditungsten(III) complex. *Beilstein J. Org. Chem.* **2018**, *14*, 2425–2434.

(20) Haberlag, B.; Wu, X.; Brandhorst, K.; Grunenberg, J.; Daniliuc, C. G.; Jones, P. G.; Tamm, M. Preparation of imidazolin-2-iminato molybdenum and tungsten benzylidyne complexes: a new pathway to highly active alkyne metathesis catalysts. *Chem. Eur. J.* **2010**, *16*, 8868–8877.

(21) Àrias, Ò.; Ehrhorn, H.; Härdter, J.; Jones, P. G.; Tamm, M. Synthesis of Ether-Functionalized and Sterically Demanding Molybdenum Alkylidyne Complexes. *Organometallics* **2018**, *37*, 4784–4800.

(22) Kugelgen, S. von; Bellone, D. E.; Cloke, R. R.; Perkins, W. S.; Fischer, F. R. Initiator Control of Conjugated Polymer Topology in Ring-Opening Alkyne Metathesis Polymerization. *J. Am. Chem. Soc.* **2016**, *138*, 6234–6239.

(23) Kugelgen, S. von; Sifri, R.; Bellone, D.; Fischer, F. R. Regioselective Carbyne Transfer to Ring-Opening Alkyne Metathesis Initiators Gives Access to Telechelic Polymers. *J. Am. Chem. Soc.* **2017**, *139*, 7577–7585.

(24) Jeong, H.; Kugelgen, S. von; Bellone, D.; Fischer, F. R. Regioselective Termination Reagents for Ring-Opening Alkyne Metathesis Polymerization. *J. Am. Chem. Soc.* **2017**, *139*, 15509–15514.

(25) Koy, M.; Elser, I.; Meisner, J.; Frey, W.; Wurst, K.; Kästner, J.; Buchmeiser, M. R. High Oxidation State Molybdenum N-Heterocyclic Carbene Alkylidyne Complexes: Synthesis, Mechanistic Studies, and Reactivity. *Chem. Eur. J.* **2017**, *23*, 15484–15490.

(26) Hauser, P. M.; Hunger, M.; Buchmeiser, M. R. Silica-Supported Molybdenum Alkylidyne N-Heterocyclic Carbene Catalysts: Relevance of Site Isolation to Catalytic Performance. *ChemCatChem* **2018**, *10*, 1829–1834.

(27) Elser, I.; Groos, J.; Hauser, P. M.; Koy, M.; van der Ende, M.; Wang, D.; Frey, W.; Wurst, K.; Meisner, J.; Ziegler, F.; Kästner, J.; Buchmeiser, M. R. Molybdenum and Tungsten Alkylidyne Complexes Containing Mono-, Bi-, and Tridentate N -Heterocyclic Carbenes. *Organometallics* **2019**, *38*, 4133–4146.

(28) Hauser, P. M.; van der Ende, M.; Groos, J.; Frey, W.; Wang, D.; Buchmeiser, M. R. Cationic Tungsten Alkylidyne N -Heterocyclic Carbene Complexes: Synthesis and Reactivity in Alkyne Metathesis. *Eur. J. Inorg. Chem.* **2020**, 1548.

(29) Chuprun, S.; Acosta, C. M.; Mathivathanan, L.; Bukhryakov, K. V. Molybdenum Benzylidyne Complexes for Olefin Metathesis Reactions. *Organometallics* **2020**, *39*, 3453–3457.

(30) Krempner, C. Role of Siloxides in Transition Metal Chemistry and Homogeneous Catalysis. *Chem. Ber.* **2011**, 1689–1698.

(31) Heppekausen, J.; Stade, R.; Goddard, R.; Fürstner, A. Practical new silyloxy-based alkyne metathesis catalysts with optimized activity and selectivity profiles. *J. Am. Chem. Soc.* **2010**, *132*, 11045–11057.

(32) Heppekausen, J.; Stade, R.; Kondoh, A.; Seidel, G.; Goddard, R.; Fürstner, A. Optimized synthesis, structural

investigations, ligand tuning and synthetic evaluation of silyloxy-based alkyne metathesis catalysts. *Chem. Eur. J.* **2012**, *18*, 10281–10299.
(33) Persich, P.; Llaveria, J.; Lhermet, R.; Haro, T. de; Stade, R.; Kondoh, A.; Fürstner, A. Increasing the structural span of alkyne metathesis. *Chem. Eur. J.* **2013**, *19*, 13047–13058.
(34) Willwacher, J.; Fürstner, A. Catalysis-based total synthesis of putative mandelalide A. *Angew. Chem. Int. Ed.* **2014**, *53*, 4217–4221.
(35) Valot, G.; Mailhol, D.; Regens, C. S.; O'Malley, D. P.; Godineau, E.; Takikawa, H.; Philipps, P.; Fürstner, A. Concise total syntheses of amphidinolides C and F. *Chem. Eur. J.* **2015**, *21*, 2398–2408.
(36) Willwacher, J.; Heggen, B.; Wirtz, C.; Thiel, W.; Fürstner, A. Total Synthesis, Stereochemical Revision, and Biological Reassessment of Mandelalide A: Chemical Mimicry of Intrafamily Relationships. *Chem. Eur. J.* **2015**, *21*, 10416–10430.
(37) Ungeheuer, F.; Fürstner, A. Concise Total Synthesis of Ivorenolide B. *Chem. Eur. J.* **2015**, *21*, 11387–11392.
(38) Ralston, K. J.; Ramstadius, H. C.; Brewster, R. C.; Niblock, H. S.; Hulme, A. N. Self-Assembly of Disorazole C1 through a One-Pot Alkyne Metathesis Homodimerization Strategy. *Angew. Chem. Int. Ed.* **2015**, *54*, 7086–7090.
(39) Hoffmeister, L.; Fukuda, T.; Pototschnig, G.; Fürstner, A. Total synthesis of an exceptional brominated 4-pyrone derivative of algal origin: an exercise in gold catalysis and alkyne metathesis. *Chem. Eur. J.* **2015**, *21*, 4529–4533.
(40) Fuchs, M.; Fürstner, A. trans-Hydrogenation: application to a concise and scalable synthesis of brefeldin A. *Angew. Chem. Int. Ed.* **2015**, *54*, 3978–3982.
(41) Schaubach, S.; Michigami, K.; Fürstner, A. Hydroxyl-Assisted trans-Reduction of 1,3-Enynes: Application to the Formal Synthesis of (+)-Aspicilin. *Synthesis* **2016**, *49*, 202–208.
(42) Meng, Z.; Souillart, L.; Monks, B.; Huwyler, N.; Herrmann, J.; Müller, R.; Fürstner, A. A "Motif-Oriented" Total Synthesis of Nannocystin Ax. Preparation and Biological Assessment of Analogues. *J. Org. Chem.* **2018**, *83*, 6977–6994.
(43) Karier, P.; Ungeheuer, F.; Ahlers, A.; Anderl, F.; Wille, C.; Fürstner, A. Metathesis at an Implausible Site: A Formal Total Synthesis of Rhizoxin D. *Angew. Chem. Int. Ed.* **2019**, *58*, 248–253.
(44) Schaubach, S.; Gebauer, K.; Ungeheuer, F.; Hoffmeister, L.; Ilg, M. K.; Wirtz, C.; Fürstner, A. A Two-Component Alkyne Metathesis Catalyst System with an Improved Substrate Scope and Functional Group Tolerance: Development and Applications to Natural Product Synthesis. *Chem. Eur. J.* **2016**, *22*, 8494–8507.
(45) Hillenbrand, J.; Leutzsch, M.; Fürstner, A. Molybdenum Alkylidyne Complexes with Tripodal Silanolate Ligands: The Next Generation of Alkyne Metathesis Catalysts. *Angew. Chem. Int. Ed.* **2019**, *58*, 15690–15696.
(46) Thompson, R. R.; Rotella, M. E.; Du, P.; Zhou, X.; Fronczek, F. R.; Kumar, R.; Gutierrez, O.; Lee, S. Siloxide Podand Ligand as a Scaffold for Molybdenum-Catalyzed Alkyne Metathesis and Isolation of a Dynamic Metallatetrahedrane Intermediate. *Organometallics* **2019**, *38*, 4054–4059.
(47) Hillenbrand, J.; Leutzsch, M.; Yiannakas, E.; Gordon, C. P.; Wille, C.; Nöthling, N.; Copéret, C.; Fürstner, A. "Canopy Catalysts" for Alkyne Metathesis: Molybdenum Alkylidyne Complexes with a Tripodal Ligand Framework. *J. Am. Chem. Soc.* **2020**, *142*, 11279–11294.
(48) Jyothish, K.; Zhang, W. Towards highly active and robust alkyne metathesis catalysts: recent developments in catalyst design. *Angew. Chem. Int. Ed.* **2011**, *50*, 8478–8480.
(49) Jin, Y.; Yu, C.; Denman, R. J.; Zhang, W. Recent advances in dynamic covalent chemistry. *Chem. Soc. Rev.* **2013**, *42*, 6634–6654.
(50) Jin, Y.; Wang, Q.; Taynton, P.; Zhang, W. Dynamic covalent chemistry approaches toward macrocycles, molecular cages, and polymers. *Acc. Chem. Res.* **2014**, *47*, 1575–1586.
(51) Yang, H.; Jin, Y.; Du, Y.; Zhang, W. Application of alkyne metathesis in polymer synthesis. *J. Mater. Chem.* **2014**, *2*, 5986.
(52) Yu, C.; Jin, Y.; Zhang, W. Shape-persistent arylene ethynylene organic hosts for fullerenes. *Chem. Rec.* **2015**, *15*, 97–106.
(53) Ortiz, M.; Yu, C.; Jin, Y.; Zhang, W. Poly(aryleneethynylene)s: Properties, Applications and Synthesis Through Alkyne Metathesis. *Top. Curr. Chem.* **2017**, *375*, 69.
(54) Ge, Y.; Huang, S.; Hu, Y.; Zhang, L.; He, L.; Krajewski, S.; Ortiz, M.; Jin, Y.; Zhang, W. Highly active alkyne metathesis catalysts operating under open air condition. *Nat. Commun.* **2021**, *12*, 1136.
(55) Lysenko, S.; Haberlag, B.; Daniliuc, C. G.; Jones, P. G.; Tamm, M. Efficient Catalytic Alkyne Metathesis with a Tri(tert-butoxy)silanolate-Supported Tungsten Benzylidyne Complex. *ChemCatChem* **2011**, *3*, 115–118.
(56) Haberlag, B.; Freytag, M.; Jones, P. G.; Tamm, M. Tungsten and Molybdenum 2,4,6-Trimethylbenzylidyne Complexes as Robust Pre-Catalysts for Alkyne Metathesis. *Adv. Synth. Catal.* **2014**, *356*, 1255–1265.
(57) Lysenko, S.; Volbeda, J.; Jones, P. G.; Tamm, M. Catalytic metathesis of conjugated diynes. *Angew. Chem. Int. Ed.* **2012**, *51*, 6757–6761.
(58) Li, S. T.; Schnabel, T.; Lysenko, S.; Brandhorst, K.; Tamm, M. Synthesis of unsymmetrical 1,3-diynes via alkyne cross-metathesis. *Chem. Commun.* **2013**, *49*, 7189–7191.
(59) Schnabel, T. M.; Melcher, D.; Brandhorst, K.; Bockfeld, D.; Tamm, M. Unraveling the Mechanism of 1,3-Diyne Cross-Metathesis Catalyzed by Silanolate-Supported Tungsten Alkylidyne Complexes. *Chem. Eur. J.* **2018**, *24*, 9022–9032.
(60) Ehrhorn, H.; Bockfeld, D.; Freytag, M.; Bannenberg, T.; Kefalidis, C. E.; Maron, L.; Tamm, M. Studies on Molybdena- and Tungstenacyclobutadiene Complexes Supported by Fluoroalkoxy Ligands as Intermediates of Alkyne Metathesis. *Organometallics* **2019**, *38*, 1627–1639.
(61) Curbet, I.; Colombel-Rouen, S.; Manguin, R.; Clermont, A.; Quelhas, A.; Müller, D. S.; Roisnel, T.; Baslé, O.; Trolez, Y.; Mauduit, M. Expedient synthesis of conjugated triynes via alkyne metathesis. *Chem. Sci.* **2020**, *11*, 4934–4938.

(62) Estes, D. P.; Bittner, C.; Àrias, Ò.; Casey, M.; Fedorov, A.; Tamm, M.; Copéret, C. Alkyne Metathesis with Silica-Supported and Molecular Catalysts at Parts-per-Million Loadings. *Angew. Chem. Int. Ed.* **2016**, *55*, 13960–13964.
(63) Estes, D. P.; Gordon, C. P.; Fedorov, A.; Liao, W.-C.; Ehrhorn, H.; Bittner, C.; Zier, M. L.; Bockfeld, D.; Chan, K. W.; Eisenstein, O.; Raynaud, C.; Tamm, M.; Copéret, C. Molecular and Silica-Supported Molybdenum Alkyne Metathesis Catalysts: Influence of Electronics and Dynamics on Activity Revealed by Kinetics, Solid-State NMR, and Chemical Shift Analysis. *J. Am. Chem. Soc.* **2017**, *139*, 17597–17607.
(64) Docherty, S. R.; Estes, D. P.; Copéret, C. Facile Synthesis of Unsymmetrical Trialkoxysilanols: (RO) 2 (R′O)SiOH. *Helv. Chim. Acta* **2018**, *101*, e1700298.
(65) Ehrhorn, H. *Katalytische Metathese von Alkinen: Entwicklung neuer Katalysatoren*; Springer, Wiesbaden (Germany), 2017.
(66) Beer, S.; Hrib, C. G.; Jones, P. G.; Brandhorst, K.; Grunenberg, J.; Tamm, M. Efficient room-temperature alkyne metathesis with well-defined imidazolin-2-iminato tungsten alkylidyne complexes. *Angew. Chem. Int. Ed.* **2007**, *46*, 8890–8894.
(67) Beer, S.; Brandhorst, K.; Hrib, C. G.; Wu, X.; Haberlag, B.; Grunenberg, J.; Jones, P. G.; Tamm, M. Experimental and Theoretical Investigations of Catalytic Alkyne Cross-Metathesis with Imidazolin-2-iminato Tungsten Alkylidyne Complexes. *Organometallics* **2009**, *28*, 1534–1545.
(68) Lysenko, S.; Daniliuc, C. G.; Jones, P. G.; Tamm, M. Tungsten alkylidyne complexes with ancillary imidazolin-2-iminato and imidazolidin-2-iminato ligands and their use in catalytic alkyne metathesis. *J. Organomet. Chem.* **2013**, *744*, 7–14.
(69) Lapadula, G.; Conley, M. P.; Copéret, C.; Andersen, R. A. Synthesis and Characterization of Rare Earth Siloxide Complexes, M[OSi(OtBu)3]3(L)x where L is HOSi(OtBu)3 and x = 0 or 1. *Organometallics* **2015**, *34*, 2271–2277.
(70) Pucino, M.; Allouche, F.; Gordon, C. P.; Wörle, M.; Mougel, V.; Copéret, C. A reactive coordinatively saturated Mo(iii) complex: exploiting the hemi-lability of tris(tert-butoxy)silanolate ligands. *Chem. Sci.* **2019**, *10*, 6362–6367.
(71) Cui, M.; Lin, R.; Jia, G. Chemistry of Metallacyclobutadienes. *Chem. Asian. J.* **2018**, *13*, 895–912.
(72) Schrock, R. R.; Jamieson, J. Y.; Araujo, J. P.; Bonitatebus, P. J.; Sinha, A.; Lopez, L.P. H. Molybdenum alkylidyne complexes that contain a 3,3′-di-t-butyl-5,5′,6,6′-tetramethyl-1,1′-biphenyl-2,2′-diolate ([Biphen]2−) ligand. *J. Organomet. Chem.* **2003**, *684*, 56–67.
(73) Àrias, Ò.; Brandhorst, K.; Baabe, D.; Freytag, M.; Jones, P. G.; Tamm, M. Formation of paramagnetic metallacyclobutadienes by reaction of diaminoacetylenes with molybdenum alkylidyne complexes. *Dalton Trans.* **2017**, *46*, 4737–4748.
(74) Haack, A.; Hillenbrand, J.; Leutzsch, M.; van Gastel, M.; Neese, F.; Fürstner, A. Productive Alkyne Metathesis with "Canopy Catalysts" Mandates Pseudorotation. *J. Am. Chem. Soc.* **2021**, *143*, 5643–5648.
(75) Addison, A. W.; Rao, T. N.; Reedijk, J.; van Rijn, J.; Verschoor, G. C. Synthesis, structure, and spectroscopic properties of copper(II) compounds containing nitrogen–sulphur donor ligands; the crystal and molecular structure of aqua[1,7-bis(N-methylbenzimidazol-2′-yl)-2,6-dithiaheptane]copper(II) perchlorate. *J. Chem. Soc., Dalton Trans.* **1984**, 1349–1356.

For Table of Contents Use: